Implementation and validation of an elastic-viscoplastic constitutive model for the analysis of geotechnical structures

João Filipe Ângelo Sio

Thesis to obtain the Master of Science Degree in Civil Engineering, Instituto Superior Técnico, University of Lisbon

Abstract. A three-dimensional elastic-viscoplastic constitutive model that is able to reproduce the time and rate dependent behaviour of soils with isotach viscosity (unique stress-strain-strain rate relationship) is presented. The constitutive law is based on the overstress theory and incorporates some noticeable features namely: (i) a versatile loading surface that is capable of reproducing a wide variety of shapes in deviatoric-mean effective stress space and (ii) assumed to be a locus of constant viscoplastic scalar multiplier to ensure that critical state conditions are reached; (iii) either a semi-logarithmic or a hyperbolic creep law that controls the development of viscoplastic deformations under isotropic stress conditions. Upon the description of the model's governing equations as well as the process of its implementation in a single stress point algorithm and in the finite difference program *FLAC 2D*, numerical analyses of common laboratory tests were performed to assess the model's potentials and limitations. The model reproduces a unique stress-strain-strain rate relationship and as such mimics well the isotach behaviour of clays; however, because of its formulation the model is unable to predict a failure load during load controlled shear test. A discussion regarding this issue is presented at the end of the work.

Keywords: constitutive relations, isotach, viscoplasticity, time and rate dependency, numerical modelling

1. Introduction

The importance of time and rate dependency of geomaterials in the design of structures, especially in the verification of the serviceability limit state, can be shown in examples such as: (a) the development of long term settlements, originating eventually internal forces and moments in the structure due to imposed differential displacements and (b) the need to plan the loading stages during construction to avoid the collapse of the structure or to limit its long-term settlements. The reproduction of these effects relies generally on sophisticated constitutive models and their complexity may increase the probability of their misuse due to the lack of understanding of the models' underlaying equations and assumptions. It is extremely important to have a clear idea about the models' strengths, weaknesses, fields of application and the behaviours that these are able to reproduce in order to perform safe and reliable engineering designs.

In this respect, the purpose of the present thesis is to give the author a better understanding on the time and rate dependent behaviour of geomaterials as well as the knowledge to reproduce correctly some of its effects through the implementation and validation of an elastic-viscoplastic constitutive model.

2. Observed time and rate dependent behaviour of soils

It is generally accepted that time and rate dependent behaviour of soils can be grouped into viscous and structuration effects [1-4]. However, one must also consider the influence of temperature given the viscous nature of geomaterials (another manifestation of the viscous nature of geomaterials [5]) and the interaction of the viscous effects with the delayed dissipation of excess pore water pressure in clayey soils.

In the past, time and rate dependency of granular geomaterials are often disregarded. However, recent studies performed by numerous of researchers [2, 6-10] showed that sand also exhibits a considerable amount of time dependent behaviour.

The viscous effects are further detailed as it includes the primary aspects intended to be reproduced by the constitutive model implemented herein.

Viscous effects are due to the viscous properties of materials and are believed to result from sliding at interparticle contacts and associated particle re-arrangement, with the presence or absence of water being insignificant [11]. Three major aspects can be observed within these effects: creep, stress relaxation and rate effects.

2.1. Creep

Creep is the prolonged deformation of the soil at constant effective stresses. In its simplest form, creep behaviour may be quantified by a relationship between strain (or void ratio) and the logarithm of time, in which the slope is characterised by a constant coefficient of secondary compression $C_{\alpha\varepsilon}$ (or $C_{\alpha e}$).

However, it is more correctly to not assume a constant coefficient of secondary compression because creep behaviour is also found to be dependent of the applied stress [12-14]; time [15-18]; level of plasticity and water content [19].

Under one dimensional conditions, soils that had been subjected to delayed compression are found to develop an apparent pre-consolidation higher than the maximum stress they had been subjected to previously [19], which can be explained by void ratio and stress history alone. Against additional loading, the soil will first behave similarly to an overconsolidated soil, being very stiff until the value of the apparent pre-consolidation pressure is exceeded. Thereafter, the soil yields and exhibits large instant deformations, joining the virgin compression line.

Later, based on the results of a series of undrained triaxial creep tests performed by Arulanandan et al. [20] (i.e. creep tests in which the deviatoric stress is maintained constant), the yield surface in three dimensional stress space was found to present similar trends in relation to the ones associated with the pre-consolidation pressure, suggesting the validity of the effects of creep in general stress space.

2.2. Stress relaxation

Stress relaxation is the continued decay in stresses at a constant level of strain. From undrained relaxation tests, Lacerda & Houston [6] observed that the ratio between the deviatoric stress at a given time and the deviatoric stress at the beginning of the stress relaxation tests varies linearly with the logarithm of time after an initial time period.

The time period necessary to initiate the decay in stress is inversely proportional to the strain rate applied prior to the relaxation process.

The slope of the observed semi-logarithmic relationship is found to be independent of the confining pressure but dependent of the initial imposed strain [6, 21]. Opposing conclusions were made concerning the existence of a limiting equilibrium stress: while Vialov & Skibitsky [22], Lacerda & Houston [6] and Akai et al. [21] did not observe a limiting equilibrium, Murayama & Shibata [23] suggested otherwise. However, given that the non-consideration of a limiting equilibrium implies a continuous decay of deviatoric stress, resulting in unrealistic stress values for prolonged relaxation tests, the consideration of a final relaxed stress level maybe more appropriate to reproduce the phenomenon.

2.3. Strain rate effects

Rate effects illustrate the change in stress-strain soil response due to the applied strain rate. Based on an extensive

laboratory testing programme, Tatsuoka [24] and co-workers have concluded that all geomaterials are affected by strain rate effects and have identified three types of viscosity behaviour: isotach, TESRA and Positive and Negative (P&N) viscosity. Two types of laboratory tests are used to study these effects: the first one termed as constant rate of strain (CRS) tests, consists on the application of a constant relevant strain rate component (vertical strain rate in oedometer tests and axial strain rate in triaxial apparatus) during the entire test procedure. The second one, named as step-wise change in the rate of strain (SRS) tests, corresponds to the application of strain rate values in a stepwise manner during a single test.

Isotach viscosity is applicable to a wide variety of clays when structuration effects do not play an important role [25]. This type of viscosity constitutes a unique stress-strain-strain rate relationship. Under one dimensional conditions, CRS tests performed by Leroueil et al. [15] revealed that, for the same level of strains, the acting stresses on a soil element are higher for faster applied strain rates. Furthermore, SRS tests performed by the same researcher showed that the effects of strain rate are permanent as long as the applied strain rate remains unchanged.

The yield surface size was found to increase with the applied strain rate [26], suggesting the extension of the isotach behaviour to general stress space.

TESRA [2, 10, 27] and P&N viscosities [28] are more commonly observed in sands but, contrary to the isotach behaviour, these are not characterised by a unique stress-strain-strain rate relationship.

It is shown that in soils with isotach viscosity creep and stress relaxation can be predicted from results of CRS tests or vice-versa, whereas in geomaterials of the TESRA and P&N type it cannot.

3. Models for time-dependent behaviour of soils

3.1. Types of models

This section aims to provide the time and rate dependent constitutive models that permitted the author to have a better understanding of the problems involved in the modelling of the behaviour of soils with isotach viscosity. According to Liingaard et al. [29], the constitutive models available from literature can be divided into three categories: empirical, rheological and general stress-strain-strain rate models. Two of the three categories are discussed herein.

3.2. Empirical models

Empirical models are mainly obtained by fitting experimental results from creep, stress relaxation and CRS tests with simple mathematical expressions based on closed form solutions or differential equations. They often reflect the real behaviour of soils, providing practical solutions to engineering problems, as long as the boundary conditions comply with laboratory experiments.

The simplest empirical models (often referred as primary empirical relations) aim to provide a quantification of the soil deformation under one dimensional conditions (1D). Examples of these models are the semi-logarithmic law, Singh & Mitchel's [16] creep model and Lacerda & Houston's [6] stress relaxation model.

Special attention is paid for the semi-logarithmic law because it serves as basis to estimate the volumetric creep deformations under isotropic stress conditions in the model implemented herein. As referred in section 2.1, the semi-logarithmic law is depicted in ε (or e) $-\log t$ space with a slope termed as the coefficient of secondary compression $C_{\alpha\varepsilon}$ (or $C_{\alpha e}$) and, depending on the approach, this slope maybe assumed as constant, stress dependent (with a constant $C_{\alpha\varepsilon}/C_{c\varepsilon}$ [12, 14]) or time dependent [17].

$$\varepsilon_z = C_{\alpha\varepsilon} \log\left(\frac{t}{t_i}\right) \tag{1}$$

where ε_z is the vertical strain.

The use of equation 1 requires the definition of the time associated with the onset of secondary compression t_i.

The empirical relations presented above only provide information regarding one component of stress and strain. Hence, researchers such as Kavazanjian & Mitchell [30] and Tavenas et al. [18] have combined these empirical relations to obtain secondary empirical models which consider both volumetric and shear strain components. This way, creep deformations can be estimated with reference to a flow rule.

The resulting empirical models still consider the delayed component of soil deformation only. In order to ensure that full soil deformation is taken into account, Bjerrum [19], Leroueil et al. [15] and Yin and Graham [31, 32] added one or more of the described empirical relations to time independent models, giving rise to the isochrone concept, strain rate approach and equivalent time concept, respectively.

3.3. General stress-strain-strain rate models

General stress-strain-strain rate models are general constitutive laws that describes not only the viscous effects but also the inviscid behaviour of soils, in principal, under any possible loading conditions. They are readily adaptable for finite element implementation because their constitutive expressions are generally given in incremental form. Special attention is paid to elastic-viscoplastic constitutive models based on the overstress theory.

The concept of overstress was developed by Perzyna [33] and considers the total strain rate to be decomposed into an elastic and viscoplastic component:

$$\{\dot{\varepsilon}^T\} = \{\dot{\varepsilon}^{el}\} + \{\dot{\varepsilon}^{vp}\} \tag{2}$$

The elastic strain rate $\{\dot{\varepsilon}^{el}\}$ is assumed to obey the generalised Hooke's law whereas the viscoplastic strain rate $\{\dot{\varepsilon}^{vp}\}$ is considered to follow the associated flow rule given by equation 3.

$$\{\dot{\varepsilon}^{vp}\} = \gamma \cdot \langle \Phi(F) \rangle \cdot \left\{\frac{\partial f_d}{\partial \sigma'_{ij}}\right\} \tag{3}$$

where $\langle \Phi(F) \rangle = \begin{cases} \Phi(F), & F > 0 \\ 0, & F \leq 0 \end{cases}$

$\{\dot{\varepsilon}^{vp}\}$ is the viscoplastic strain rate tensor; σ'_{ij} is the effective stress tensor; γ is a fluidity parameter; $\Phi(F)$ is the viscoplastic multiplier and a function of the overstress, F, the quantity F being defined as the normalised distance between the current dynamic loading surface, f_d, and the static loading surface, f_s, which defines the region of time-independent and purely elastic behaviour (i.e. a yield surface):

$$F = \frac{f_d}{f_s} - 1 \tag{4}$$

The overstress theory differs from the classic plasticity theory in the sense that it does not invoke the consistency rule in the derivation of the theory. While in the classic plasticity theory the magnitude of inelastic strains is related to stress rate and current stress state, in the overstress theory, this is related to the current stress state only, and independent of stress rate or stress history. Furthermore, because the consistency rule is not assumed in the theory, the stress state can lie within, on and above the static yield surface.

It can be shown that the overstress theory is able to mimic permanent strain rate effects in a material's stress-strain response and is able to simulate the phenomena of creep and stress relaxation provided that the processes start from a stress state above the static yield surface f_s. However, as shown by Adachi et al. [34], it lacks the capability to model tertiary creep (creep rupture) due to its formulation.

The value of $\Phi(F)$ may be evaluated by curve fitting the results obtained from laboratorial tests [e.g. 8] and, according to Liingaard et al. [29], two of the most used forms are:

$$\Phi(F) = aF^6 \quad and \quad \Phi(F) = c \cdot \exp(jF^k) - 1 \tag{5}$$

where a, b, c, j and k are constants.

An alternative approach to evaluate $\Phi(F)$ used by researchers such as Adachi et al. [34], Yin et al. [35] and Bodas Freitas et al. [36, 37] is to replace the static yield surface with a reference loading surface f_{ref} associated with a finite viscoplastic strain rate value.

The approach considers one of the empirical creep laws presented in 3.2. However, since these laws are only valid under isotropic stress conditions, the model evaluate first the volumetric viscoplastic strain rate instead. The viscoplastic behaviour is then extended to generalised stress space based on further assumptions regarding the ratio between the volumetric and the deviatoric viscoplastic strain increments. Bodas Freitas et al. [37] showed that the correct assumption to this is to consider the loading surface as a locus of constant $\Phi(F)$.

A static or limiting surface may exist or not depending on the creep law being applied. If the empirical creep law imposes no limiting surface, $\Phi(F)$ is always evaluated and the model predicts an infinite viscoplastic strain at infinite creep time under constant effective stresses. Conversely, if a limiting surface is specified then it defines the region of pure elastic behaviour, in which $\Phi(F)$ is not evaluated.

4. Model description and implementation

4.1. Stress and strain invariants

The constitutive model is mostly presented in terms of individual stress and strain components. However, it is usually convenient to separate the response of the model into its volumetric and deviatoric components with the use of invariants. In this respect, the stress invariants considered in this work are the mean effective stress p', the deviatoric stress q and the Lode's angle θ, given by equations 6 to 8, respectively.

$$p' = \frac{1}{3}\left(\sigma'_{xx} + \sigma'_{yy} + \sigma'_{zz}\right) \tag{6}$$

$$q = \left[\frac{3}{2}\left(s_{ij} : s_{ij}\right)\right]^{1/2} \tag{7}$$

$$\theta = \frac{1}{3}\sin^{-1}\left[-\frac{27}{2}\cdot\frac{\det\left(s_{ij}\right)}{q^3}\right] \tag{8}$$

where s_{ij} is the deviatoric stress tensor, its components being calculated as shown in equation 9.

$$s_{ij} = \sigma'_{ij} - p' \cdot \delta_{ij} \tag{9}$$

where σ'_{ij} is the effective stress tensor and δ_{ij} is the Kronecker's delta.

Instead of using the Lode's angle it is often more convenient to use as a stress invariant the quantity z which is taken as $\sin 3\theta$.

$$z = \sin 3\theta = -\frac{27}{2}\cdot\frac{\det\left(s_{ij}\right)}{q^3} \tag{10}$$

The volumetric and deviatoric strain invariants, expressed in incremental form, are given by equations 11 and 12, respectively.

$$\Delta\varepsilon_{vol} = \Delta\varepsilon_{xx} + \Delta\varepsilon_{yy} + \Delta\varepsilon_{zz} \tag{11}$$

$$\Delta E_d = \left[2\left[\begin{array}{c}\left(\Delta\varepsilon_{xx} - \frac{\Delta\varepsilon_{vol}}{3}\right)^2 + \left(\Delta\varepsilon_{yy} - \frac{\Delta\varepsilon_{vol}}{3}\right)^2 \\ + \left(\Delta\varepsilon_{zz} - \frac{\Delta\varepsilon_{vol}}{3}\right)^2 + \frac{1}{2}\left(\Delta\gamma_{xy}^2 + \Delta\gamma_{yz}^2 + \Delta\gamma_{zx}^2\right)\end{array}\right]\right]^{1/2} \tag{12}$$

where $\Delta\varepsilon_{vol}$ is the volumetric strain invariant and ΔE_d is the volumetric stress invariant.

Compressive stresses and strains are assumed as positive.

4.2. Evaluation of the strain increment

In a typical elastic-viscoplastic model, the soil strain increment (equation 13) is divided into two parts: an elastic part which is instantaneous and time independent, and a viscoplastic part which is time dependent and irreversible.

$$\{\Delta\varepsilon^T\} = \{\Delta\varepsilon^{el}\} + \{\Delta\varepsilon^{vp}\} \tag{13}$$

The elastic strain increment vector can be determined by inverting equation 14.

$$\{\Delta\sigma'\} = [D']\{\Delta\varepsilon^{el}\} \tag{14}$$

where $[D']$ is the elastic constitutive matrix. The elastic response is assumed to be isotropic and is fully characterised by two elastic parameters, a stress dependent bulk modulus (defined by equation 15) and a second elastic parameter that can either be the Poisson's ratio v or the elastic shear modulus G.

$$K' = \frac{\kappa}{Vp'} \tag{15}$$

Based on Perzyna's overstress theory, the viscoplastic strain increment $\{\Delta\varepsilon^{vp}\}$ is given as:

$$\{\Delta\varepsilon^{vp}\} = \{\dot{\varepsilon}^{vp}\}\cdot\Delta t = \langle\Phi\rangle\cdot\left\{\frac{\partial f_d}{\partial\sigma'_{ij}}\right\}\cdot\Delta t \tag{16}$$

where $\langle\Phi\rangle = \begin{cases}\Phi, & soil\ state\ above\ the\ yield\ surface\\ 0, & soil\ state\ below\ the\ yield\ surface\end{cases}$

$\{\dot{\varepsilon}^{vp}\}$ is the viscoplastic strain rate tensor; Φ is the viscoplastic scalar multiplier; f_d is the current dynamic loading surface; σ'_{ij} is the effective stress state and Δt is the time increment.

A non-associated flow rule may be considered, in which case the potential used to define the direction of the viscoplastic strain vector is different from the dynamic loading surface and the resulting expression for the viscoplastic strain increment would be then given in equation 17.

$$\{\Delta\varepsilon^{vp}\} = \langle\Phi\rangle\cdot\left\{\frac{\partial g}{\partial\sigma'_{ij}}\right\}\cdot\Delta t \tag{17}$$

where g is the plastic potential, in principle different from f_d, $\{\partial g/\partial\sigma'_{ij}\}$ is the derivative of the plastic potential in order to the six stress components (also known as the directional component of the viscoplastic strain increment tensor).

The plastic potential g and the viscoplastic scalar multiplier Φ are subsequently derived.

4.3. Plastic potential and loading surface

The surface proposed by Lagioia et al. [38] is used herein:

$$f\ or\ g = \frac{p'}{p'_c} - \frac{\left(1+\frac{q}{K_2 M(\theta)p'}\right)^{\frac{K_2}{(1-\mu)(K_1-K_2)}}}{\left(1+\frac{q}{K_1 M(\theta)p'}\right)^{\frac{K_1}{(1-\mu)(K_1-K_2)}}} = 0 \tag{18}$$

where p'_c is the mean effective stress at $q = 0$ (i.e. the pre-consolidation pressure) and the constants K_1 and K_2 are given by equation 19.

$$K_{1/2} = \frac{\mu(1-\alpha)}{2(1-\mu)}\left(1 \pm \sqrt{1 - \frac{4\alpha(1-\mu)}{\mu(1-\alpha)^2}}\right) \tag{19}$$

where μ and α are model parameters and $M(\theta)$ is given by the failure criterion in the deviatoric plane proposed by Van Eekelen [39]:

$$M(\theta) = \alpha_{VE}(1 - z\beta_{VE})^n \tag{20}$$

where n is the parameter that represents the type of surface being used, z is the invariant associated to the Lode's angle, α_{VE} and β_{VE} are the parameters to fit measured values of the angle of shear resistance, φ', at two values of θ, for any type of soils. In this case, α_{VE} and β_{VE} were used to fit the stress ratios at failure under triaxial compression and extension, corresponding to a value of $z = -1$ and $z = 1$, respectively.

$$\alpha_{VE} = \frac{M_c}{2^n}\left(1 + r_m^{1/n}\right)^n \tag{21}$$

$$\beta_{VE} = \frac{1 - r_m^{1/n}}{1 + r_m^{1/n}} \tag{22}$$

where r_m is the ratio of M_e to M_c, being M_e and M_c the slope of the Critical State Line (CSL) in $q - p'$ stress space under triaxial extension and compression, respectively. M_c is shown to be related to the angle of shear resistance φ'_c as follows:

$$M_c = \frac{6 \sin \varphi'_c}{3 - \sin \varphi'_c} \tag{23}$$

Equation 18 was obtained by integrating the relationship between the dilatancy d (the ratio of volumetric to deviatoric plastic strain increment) and the stress ratio $\eta = q/p'$. It ensures that the dilatancy ratio is zero at the critical state and infinite under isotropic stress conditions (i.e. only incremental volumetric viscoplastic strains are predicted). The surface is versatile in the sense that the user is able to define different types of $d - \eta$ curves by calibrating the parameters μ and α. It breaks the link between the undrained shear strength and the angle of shear resistance, enabling one to prevent the model from overestimating the undrained shear strength by changing the surface's shape.

To fully define the loading surface (or plastic potential), five parameters are required: M_c, μ, α, r_M and p'_c. The first four quantities are model parameters and p'_c defines the size of the loading surface which depends on the current stress state.

4.4. Derivation of Φ for the model with the semi-logarithm creep law

The viscoplastic scalar multiplier Φ can be derived based on the following steps for both creep laws:

1) Find the appropriate expression for the volumetric viscoplastic strain rate that takes into account the assumed stress-strain-strain rate relationship under isotropic stress conditions;

2) Then, assuming the loading surface as a locus of constant Φ, extend the viscoplastic behaviour to general stress space in order to obtain the viscoplastic scalar multiplier.

The model framework under isotropic stress conditions applied for each creep law is slightly different. Figure 1 illustrates the behaviour assumed in the model that incorporates the semi-logarithm creep law, in which the time-dependent deformations of a soil element under constant isotropic effective stresses at time interval t is described by equation 24.

$$\varepsilon_{vol}^{vp} = -\frac{\Delta e}{1 + e} = \frac{\psi}{1 + e} \cdot \ln\left(\frac{t}{t_0}\right) \tag{24}$$

where t_0 is the time associated with the onset of secondary compression (conventionally taken as 1.0 day for normally consolidated states), ψ is the creep parameter and e is the current void ratio.

Differentiating equation 24 in order to time gives the volumetric viscoplastic strain rate (assuming compression positive).

$$\dot{\varepsilon}_{vol}^{vp} = \frac{\psi}{1 + e} \cdot \frac{1}{t} \tag{25}$$

Equation 25 implies the existence of a family of normal compression lines (NCL), each corresponding to a certain loading time t or volumetric viscoplastic strain rate. NCLs are assumed to plot as straight lines with slope λ in $V - \ln p'$ space, just as shown in figure 1.

The reference NCL corresponds to a time $t = t_0$ and a volumetric viscoplastic strain rate $\dot{\varepsilon}_{vol}^{vp} = \dot{\varepsilon}_{vol}^{ref}$.

The instant line characterises the instant elastic response of the soil and is plotted as a straight line with slope κ in $V - \ln p'$ space (also shown in figure 1).

The use of equations that are expressed as a function of time, such as equations 24 and 25 requires the definition of a reference for time, which is not so straightforward. Therefore, it is more convenient to express the volumetric viscoplastic strain rate as a function of its current state instead.

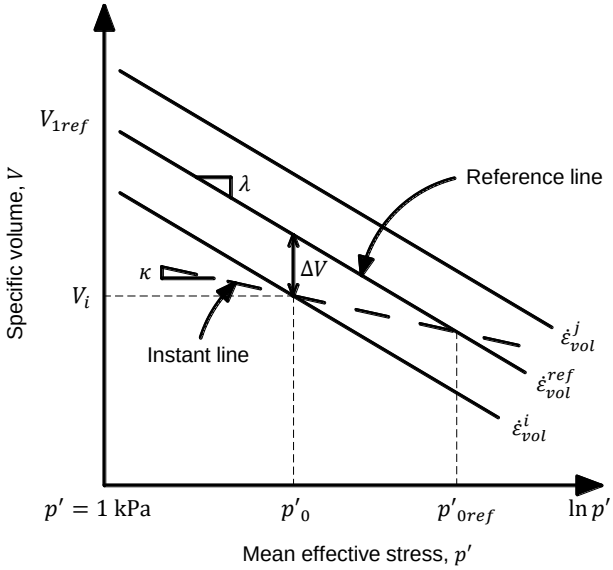

Figure 1 – Schematic representation of the time-dependent behaviour under isotropic stress conditions for the semi-logarithm creep law [37]

At instant t, after the application of a constant isotropic effective stress p'_0, the specific volume V_i can be given as:

$$V_i = V_{1ref} - (\lambda - \kappa) \ln p'_{0ref} - \kappa \ln p'_0 \tag{26}$$

or as:

$$V_i = V_{1ref} - \lambda \ln p'_0 + \Delta V \tag{27}$$

where V_{1ref} is the specific volume at unit mean effect stress on the reference NCL, p'_{0ref} is the mean effective stress at the intersection of the instant line that passes through the current state and the reference NCL and ΔV, which is given by equation 28, is the variation of the specific volume due to time-dependent deformation under constant mean effective stress (i.e. the vertical measure between the reference and current NCLs).

$$\Delta V = \Delta e = -\varepsilon_{vol}(1 + e) = -\psi \cdot \ln\left(\frac{t}{t_0}\right) \tag{28}$$

Substituting equation 25 into equation 28 for both current and reference times gives:

$$\Delta V = \psi \cdot \ln\left(\frac{\dot{\varepsilon}_{vol}^{i}}{\dot{\varepsilon}_{ref}^{i}}\right) \tag{29}$$

Eliminating the quantities V_i and V_{1ref} by combining equations 26 and 27, the volumetric viscoplastic strain rate is obtained.

$$\dot{\varepsilon}_{vol}^{vp} = \dot{\varepsilon}_{vol}^{ref}\left(\frac{p'_0}{p'_{0ref}}\right)^{\frac{\lambda-\kappa}{\psi}} = \frac{\psi}{1 + e}\frac{1}{t_0}\left(\frac{p'_0}{p'_{0ref}}\right)^{\frac{\lambda-\kappa}{\psi}} \tag{30}$$

According to this model formulation, the stress path moves along the current instant time line for a given mean effective stress increment and, as a response of the soil, an associated elastic volumetric strain increment is developed. Then, with time t, under constant mean effective stress, delayed volumetric viscoplastic strain increments will bring the stress state to the appropriate compression line and the value of p'_{0ref} is updated as follows:

$$\Delta p'_{0ref} = p'_{0ref}\frac{V}{\lambda - \kappa}\Delta\varepsilon_{vol}^{vp} \tag{31}$$

where $\Delta\varepsilon_{vol}^{vp}$ is the viscoplastic volumetric strain increment.

It is now required to extend the constitutive model to general stress space in order to obtain the viscoplastic scalar multiplier. The current loading surface is a surface characterised by a

certain mean effective stress at zero deviatoric stress p'_0 that passes through the current stress state ($p' = p'_i$ and $q = q_i$). Assuming that Φ is constant on the current loading surface, this can be determined noting that the volumetric viscoplastic strain rate under isotropic stress conditions (at $p' = p'_0$ and $q = 0$) can be calculated using either equation 17 or 30.

$$\Delta\varepsilon^{vp} = \dot{\varepsilon}_{vol}^{ref}\left(\frac{p'_0}{p'_{0ref}}\right)^{\frac{\lambda-\kappa}{\psi}} \cdot \Delta t = \Phi \cdot \left|\frac{\partial g}{\partial p'}\right|_{\substack{p'=p'_0 \\ q=0}} \cdot \Delta t \qquad (32)$$

Rearranging equation 32, the expression for Φ is given as:

$$\Phi = \frac{\psi}{1+e} \cdot \frac{1}{t_0} \cdot \left(\frac{p'_0}{p'_{0ref}}\right)^{\frac{\lambda-\kappa}{\psi}} \Bigg/ \left|\frac{\partial g}{\partial p'}\right|_{\substack{p'=p'_0 \\ q=0}} \qquad (33)$$

The introduction of the absolute value of $\partial g/\partial p'$ is to ensure that Φ is always positive. Equation 34 gives the value of $|\partial g/\partial p'|$ evaluated at the equivalent isotropic stress state.

$$\left|\frac{\partial g}{\partial p'}\right|_{\substack{p'=p'_0 \\ q=0}} = \left|\frac{1}{p'_0}\right| \qquad (34)$$

Equation 33 indicates that Φ is related to the horizontal distance between the quantities p'_0 and p'_{0ref} and the locus of points where volumetric strains are purely elastic is inexistent because volumetric viscoplastic strains are always developed (i.e. no limit of volumetric viscoplastic strain is imposed in the equation).

To this end, the problem of evaluating Φ at general stress state is reduced to evaluating it at the equivalent isotropic state (i.e. at $p' = p'_0$ and $q = 0$).

Based on the assumption that the loading surface and the plastic potential coincides, 9 input parameters are needed for the semi-logarithm creep law model.

In addition, one needs to specify the initial stresses, the void ratio, e_0, and the overconsolidation ratio (OCR) to initialise the numerical model. Note that the overconsolidation ratio is defined in relation to the reference NCL.

For further details concerning the quantification of the model parameters, please refer to the main document.

4.5. Derivation of Φ for the model with the hyperbolic creep law

The schematic representation of the model framework under isotropic stress conditions suited for the hyperbolic creep law is presented in figure 2. The equivalent time concept is invoked to overcome the problems that arise when the soil's delayed compression is related to time (i.e. the same problem discussed in 4.4).

Equivalent time lines are a family of normal compression lines with slope λ/V in $\varepsilon_{vol} - \ln p'$ space, each of these corresponding to an equivalent time t_e. Equivalent time t_e is the time that a soil element would take to creep from the reference compression line to the current stress state under constant mean effective stress. Equivalent time t_e as a rule does not correspond to the real time.

Reference compression line (or reference time line) corresponds to the NCL with zero equivalent time and, given that the strain origin is arbitrary, it is assumed to pass through the point ($\varepsilon_{vol} = 0$; $p' = 1$ kPa). It corresponds to the soil's isotropic normal compression line and is associated with a real loading time t_0 (conventionally taken as 1 day).

Soil states below the reference compression line assume positive equivalent times ranging from zero to infinite and equivalent times above the reference compression line varies between zero and the value of $-t_0$.

Equivalent times can also be shown to be directly related to unique volumetric viscoplastic strain rates, with large equivalent times being associated to smaller volumetric viscoplastic strain rates.

A limit time line spaced from the reference time line by a vertical distance of $\varepsilon_{vol,m,Limit}^{vp}$ is considered. The limit time line defines the region of stress states attained after an infinite time of drained creep; stress states located on or under this limit are heavily consolidated, developing elastic deformations only. The limit time line constitutes a yield surface.

The elastic line characterises the instant elastic response of the soil and is plotted as a straight line with slope κ/V in $\varepsilon_{vol} - \ln p'$ space.

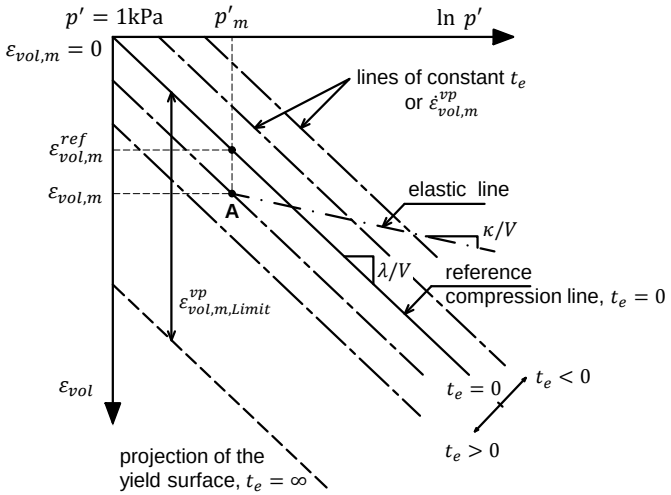

Figure 2 – Schematic representation of the time-dependent behaviour under isotropic stress conditions for the hyperbolic creep law [36]

With reference to figure 2, the volumetric strain of a given soil under a mean effective stress, p'_m, is given as:

$$\varepsilon_{vol,m} = \varepsilon_{vol,m}^{ref} + \varepsilon_{vol,m}^{vp} \qquad (35)$$

where $\varepsilon_{vol,m}^{ref}$ is the volumetric strain at the reference NCL and $\varepsilon_{vol,m}^{vp}$ is the volumetric viscoplastic strain (i.e. the vertical distance between the reference and the current loading NCL).

Yin [17] proposed the following non-linear creep law to quantify the volumetric viscoplastic strains:

$$\varepsilon_{vol,m}^{vp} = \frac{\frac{\psi_0}{V}\ln\left(\frac{t_0+t_e}{t_0}\right)}{1+\frac{\psi_0}{V\cdot\varepsilon_{vol,m,Limit}^{vp}}\ln\left(\frac{t_0+t_e}{t_0}\right)} \qquad (36)$$

where t_0 is the real time associated to the reference time line; t_e is the equivalent time that the soil needs to creep from the reference to the current loading NCL; ψ_0/V is the constant associated to the creep parameter and $\varepsilon_{vol,m,Limit}^{vp}$ is the limit of volumetric viscoplastic strain.

Based on equations 35 and 36, the resulting volumetric viscoplastic strain rate can be shown to be given as:

$$\dot{\varepsilon}_{vol,m}^{vp} = \frac{\psi_0}{V\cdot t_0}\cdot\left(1+\frac{\varepsilon_{vol,m}^{ref}-\varepsilon_{vol,m}}{\varepsilon_{vol,m,Limit}^{vp}}\right)^2 \times \exp\left[\frac{V}{\psi_0}\frac{\varepsilon_{vol,m}^{ref}-\varepsilon_{vol,m}}{\left(1+\frac{\varepsilon_{vol,m}^{ref}-\varepsilon_{vol,m}}{\varepsilon_{vol,m,Limit}^{vp}}\right)}\right] \qquad (37)$$

The extension to general stress space follows the same procedure specified for the semi-logarithm creep law model. Φ is expressed as:

Table 1 – Model parameters set for the semi-logarithm model to predict simple laboratory tests

M_c	r_m	κ	λ	ν	α	μ	ψ_0
1.2	0.714	0.021	0.21	0.25	0.4	0.9	0.011

Table 2 – Model parameters set for the hyperbolic model to predict simple laboratory tests

M_c	r_m	κ/V	λ/V	ν	α	μ	ψ_0/V	$\varepsilon_{vol,m,Limit}^{vp}$
1.2	0.714	0.0084	0.084	0.25	0.4	0.9	0.0044	0.06

Table 3 – Initial state of the soil (stress values in kPa)

e_0	OCR with reference to the reference time line	σ'_{xx}	σ'_{yy}	σ'_{zz}	τ_{xy}	τ_{yz}	τ_{zx}
1.5	1.0	600	600	600	0	0	0
	1.5	400	400	400	0	0	0
	4.0	150	150	150	0	0	0

$$\Phi = \frac{\psi_0}{V \cdot t_0} \cdot \left(1 + \frac{\varepsilon_{vol,m}^{ref} - \varepsilon_{vol,m}}{\varepsilon_{vol,m,Limit}^{vp}}\right)^2 \times \exp\left[\frac{V}{\psi_0} \frac{\varepsilon_{vol,m}^{ref} - \varepsilon_{vol,m}}{\left(1 + \frac{\varepsilon_{vol,m}^{ref} - \varepsilon_{vol,m}}{\varepsilon_{vol,m,Limit}^{vp}}\right)}\right] \times \frac{1}{\left|\frac{\partial g}{\partial p'}\right|_{\substack{p'=p'_m \\ q=0}}} \quad (38)$$

where $|\partial g/\partial p'|_{\substack{p'=p'_m \\ q=0}} = |1/p'_m|$, being p'_m the current loading pre-consolidation pressure.

The overstress is now the vertical measure from the current loading NCL to both the reference NCL and the limit time line.

The application of equation 38 requires the knowledge of the value of the current pre-consolidation pressure p'_m (the mean effective stress at $q = 0$ on the current loading surface) and of the current value of ε_{vol} which can be determined by means of equation 39. At the start of the analyses, the initial value of ε_{vol} can be calculated with equation 40 and is constantly updated by accumulating the total volumetric strain obtained during the stepping process.

$$\varepsilon_{vol,m} = \varepsilon_{vol} - \frac{\kappa}{V} \ln\left(\frac{p'_i}{p'_m}\right) \quad (39)$$

where ε_{vol} is the current accumulated volumetric strain. In the beginning of the analysis, the initial value of ε_{vol} is calculated using the following equation:

$$\varepsilon_{vol} = \frac{\lambda}{V} \ln\left(\frac{p'_{mc}}{1\ kPa}\right) - \frac{\kappa}{V} \ln\left(\frac{p'_{mc}}{p'_i}\right) \quad (40)$$

where p'_{mc} is the largest NC stress state that the soil has experienced and can be obtained with the initial stress state, the OCR and the model parameters.

Based on the assumption that the loading surface and the plastic potential coincides, 10 input parameters are needed for the hyperbolic creep law model. For further details concerning the quantification of the model parameters, please refer to the main document.

4.6. Implementation of the model in a single stress point algorithm and in FLAC 2D

A 3rd order Runge-Kutta integration scheme with an error controlled sub-stepping was applied to estimate approximately the non-linear stress increment of the soil in response to a given total strain increment.

The total strain increment is obtained differently depending on which program the model is implemented.

Since the increment variable is a given load or displacement in the single stress point algorithm, the total strain increment must be calculated using Bardet and Choucair's [40] linearised constraints technique. It consists on the principle of linearising the loading constraints of simple laboratoy tests and linking these to the constitutive relations to form a linear system of ordinary differential equations. These equations are then integrated with the implemented integration scheme.

The total strain increments $\{\Delta\varepsilon^T\}$ can be shown to be calculated with equation 41:

$$\{\Delta\varepsilon^T\} = ([S][D] + [E])^{-1} \cdot (\{\Delta Y\} + [S][D]\{\Delta\varepsilon^{vp}\}) \quad (41)$$

where $\{\Delta\varepsilon^{vp}\}$ is the viscoplastic strain increment, $[D]$ is the elastic constitutive matrix, $\{\Delta Y\}$ is the driving variable (given by equation 42), $[S]$ and $[E]$ are the matrices that represents the stress and strain constraints of a given laboratory tests, respectively (i.e. boundary conditions).

$$\{\Delta Y\} = \{0 \quad 0 \quad 0 \quad 0 \quad 0 \quad \Delta X\}^T \quad (42)$$

where ΔX is the increment of the given load or strain component.

Stress increments are then calculated using equation 43.

$$\{\Delta\sigma'\} = [D'](\{\Delta\varepsilon^T\} - \{\Delta\varepsilon^{vp}\}) \quad (43)$$

In the finite difference program *FLAC 2D*, the increment variable is already a strain increment and stress increments maybe directly calculated using equation 43 upon estimating the viscoplastic strain increments.

5. Numerical analyses of simple laboratory tests

Four types of laboratory tests are simulated for both semi-logarithm and hyperbolic model:

a) Strain controlled drained triaxial compression tests;
b) Strain controlled undrained triaxial compression tests;
c) Strain controlled oedometer tests;
d) Drained creep tests under isotropic stress conditions;

The effects of strain rate are studied with tests a), b) and c) on samples with OCR of 1.0, 1.5 and 4.0 (with reference to the reference time line) and by applying a strain rate of 1%, 10% and 100% strain per day. Type d) tests study the performance of the model during a creep period on a sample with an OCR equal to 1.0.

Tables 1 and 2 give the model parameters set for the semi-logarithm and the hyperbolic model, respectively. Unless stated otherwise, the values set for ψ_0, ψ_0/V and $\varepsilon_{vol,m,Limit}^{vp}$ are taken as the ones given in these tables. Table 3 gives the initial state of the soil.

Figures 3(a) and (b) show the predictions of CRS oedometer tests with applied total vertical strain rates of 1%, 10% and 100% strain per day on a sample with an initial OCR equal to 4.0 (isotropically consolidated to 150 kPa) given by the EVP model with both the semi-logarithm and the hyperbolic creep laws, in the single stress point algorithm (*MATLAB*) and in *FLAC 2D*.

The figures evidence the behaviour of a soil element with isotach viscosity as these illustrate the increase in the apparent yield stress of the soil element with faster applied strain rates.

The increase may be interpreted as an increase in pseudo-elastic regime the soil acquires: stress state travels further on the recompression line in $V - \ln p'$ space before bending towards the K_0 relationship due to the development of greater viscoplastic strains in each step increment. Assuming that the

same strain increment per step is considered in the various simulations, the time step Δt decreases with faster applied strain rates, reducing the subtractive component of equation 44. Consequently, higher stress increments are predicted by the equation.

$$\{\Delta\sigma'\} = [D]\left(\{\Delta\varepsilon^T\} - \langle\Phi\rangle \cdot \left\{\frac{\partial g}{\partial \sigma'_{ij}}\right\} \cdot \Delta t\right) \qquad (44)$$

Stress state remains on the stress path that corresponds to the applied strain rate with continued straining, highlighting the permanency of the effects of strain rate on the response of the soil.

The comparison of the set of stress paths between the semi-logarithm and hyperbolic models in $V - \ln p'$ space shows the underlaying characteristics of the implemented creep laws. The vertical spacing between these is constant in the semi-logarithm model and monotonically increasing for higher applied strain rates in the hyperbolic model, representing implicitly their respective creep behaviour depicted in $\varepsilon_{vol} - \ln t$ diagram: linear relationship for the former and non-linear for the latter.

The value of the vertical spacing is controlled by the creep parameter, ψ_0 or ψ_0/V depending on the model, whereas the rate at which that spacing increases for faster applied strain rates (observed in the hyperbolic model) is governed by the limit of volumetric viscoplastic strain, $\varepsilon_{vol,m,Limit}^{vp}$.

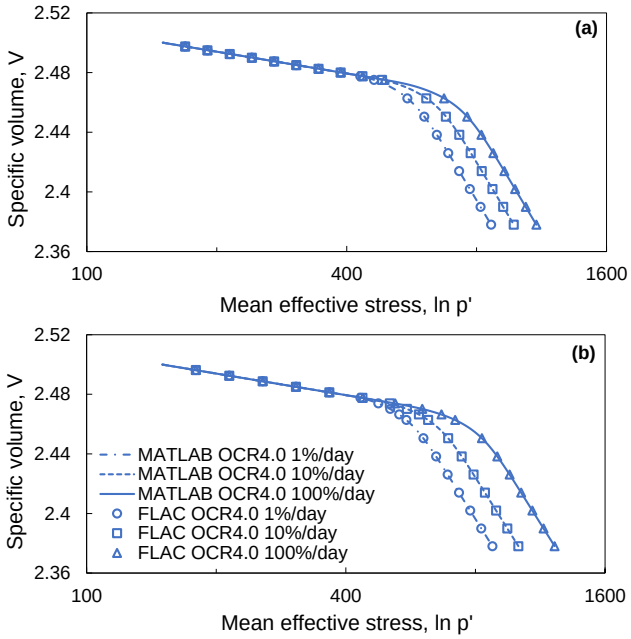

Figure 3 – CRS oedometer tests with applied strain rates of 1%, 10% and 100% strain per day on a sample with an OCR equal to 4.0: (a) semi-log model in $V - \ln p'$ space and (b) hyperbolic model in $V - \ln p'$ space (stress values in kPa)

Figures 4(a) to (c) give the hyperbolic model prediction of CRS undrained triaxial compression tests with 1%, 10% and 100% applied strain per day on samples with 1.0, 1.5 and 4.0 OCR.

Figures 4(a) and (c) indicate the increase in undrained shear strength with faster applied strain rates. However, since the effective stress critical envelop (represented by the CSL) remains unchanged in $q - p'$ space, the increase is owed to the development of lower creep induced pore water pressures at critical state, the evidence being shown in figure 4(b).

With a reduction in the applied strain rate the soil has more time to develop delayed volumetric deformations. If drainage was allowed, the increase in delayed volumetric deformations would cause the soil to contract, but since undrained conditions are imposed, extra pore water pressures are generated instead, reducing the acting mean effective stress and the undrained shear strength of the soil.

The increase in undrained shear strength with faster applied strain rates suggests the inability of the model to reproduce soil failure due to incremental load or creep rupture. As strain rate increases drastically in the imminence of collapse, the model predicts an increase in the undrained shear strength which will surpass the current total sustained load and prevent the failure. Further studies concerning this aspect are presented in section 6.

Similar to the results of CRS oedometer tests, it is possible to observe the larger pseudo-elastic regime the soil acquires in figures 4(a) to (c): stress state travels longer on the vertical line in $q - p'$ space due to the increase in surface's size, generating more pore water pressure as shown in $pp - \varepsilon_a$ space. Furthermore, the set of stress paths for soil elements with an initial OCR equal to 1.5 highlights the change in soil behaviour with applied strain rate. Contractive behaviour is predicted for 1% and 10% applied strain per day and dilative behaviour for 100% applied strain per day. An increase in the applied strain rate suggests an increase of the apparent OCR of the soil.

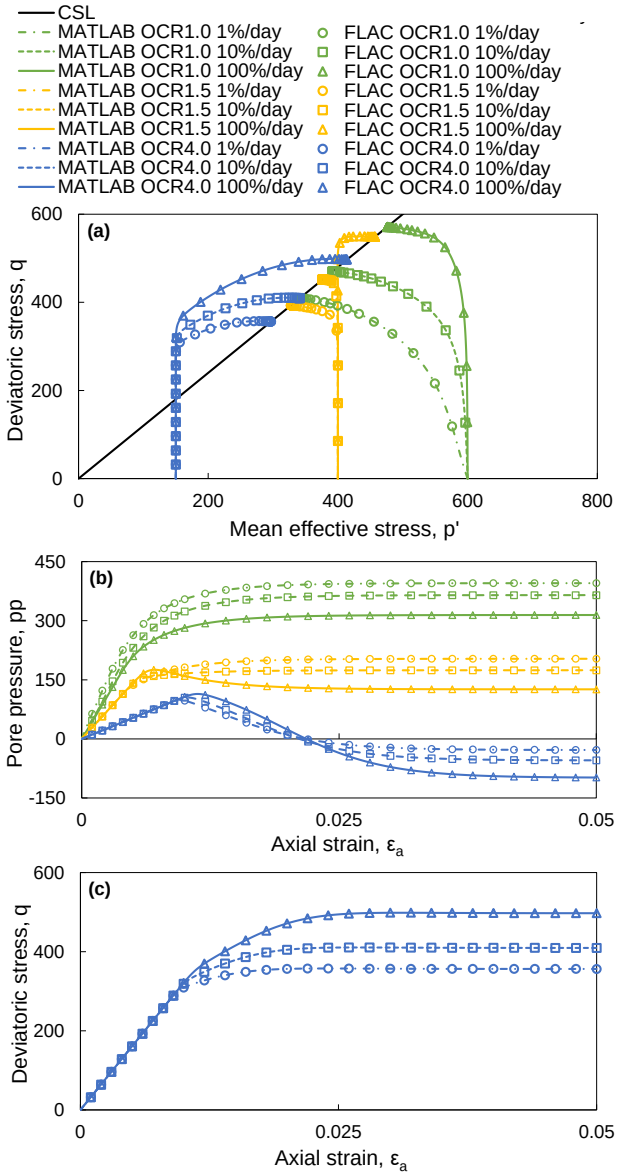

Figure 4 – Hyperbolic prediction of CRS undrained triaxial compression tests with 1%, 10% and 100% applied strain per day on samples with 1.0, 1.5 and 4.0 OCR in: (a) $q - p'$; (b) $pp - \varepsilon_a$ and (c) $q - \varepsilon_a$ space (stress values in kPa)

The uniqueness of the CSL is investigated. Results from drained triaxial compression tests showed that the CSL in $q - p'$ space is unique regardless of the applied strain rate. All three stress paths present the same value of q and p' at the critical state. Hence, the angle of shear resistance is rate independent

and an increase in its value would imply the development of structuration. However, the projection of the CSL in $V - \ln p'$ space is found to be dependent of the applied strain rate. Soil state attains higher values of specific volume at the critical state for faster applied strain rates, the increase being approximately 0.025 per logarithm cycle of strain rate.

Sorensen [41] and Bodas Freitas et al. [36] indicated that existing laboratory data corroborates the uniqueness of the CSL in $q - p'$ space but is inconclusive about its non-uniqueness in $V - \ln p'$ space because the variance of the specific volume per logarithm cycle of strain rate is within the expected scatter of the experimental measurements.

Figure 5 shows the results of a series of drained creep tests under isotropic stress conditions on a normally consolidated sample isotopically consolidated to 600 kPa in $\varepsilon_{vol} - \log t$ space, predicted by the semi-logarithm and hyperbolic creep laws. For the analysis using the hyperbolic creep law, the limit of volumetric viscoplastic strain was varied from 0.06 to 10000.

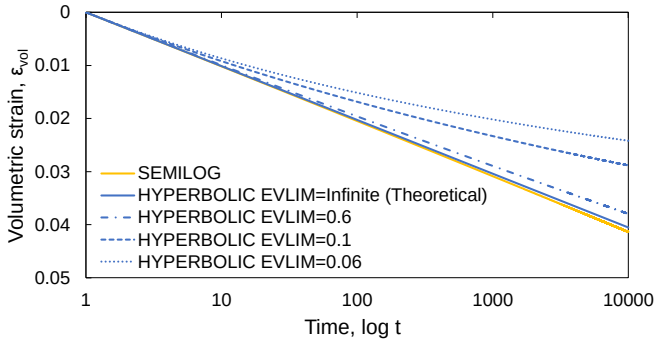

Figure 5 – Drained creep tests under isotropic stress conditions on a normally consolidated sample with a pre-consolidation pressure of 600 kPa predicted by the semi-logarithm and the hyperbolic models (time in days)

Figure 5 supports that the hyperbolic creep law gives predictions very close to the semi-logarithm creep law when a large limit of volumetric viscoplastic strain is adopted; the approximation increasing for larger limit of volumetric viscoplastic strain.

One may expect a perfect overlay of the creep laws when a sufficiently large value is adopted for the limit of volumetric viscoplastic strain. However, this is not the case; as shown in figure 5 the semi-logarithm creep law deviates slightly from the perfect linear relationship which is obtained by the hyperbolic model with a limit equal to infinite (this data series was obtained analytically).

This deviation is due to the fact that the two creep laws are defined in different spaces: in the semi-logarithm model it is assumed that the creep parameter ψ_0 is constant, while in the hyperbolic model a constant value of ψ_0/V is considered instead. In addition, a large displacement approach is used when updating the current specific volume.

Therefore, the difference between the slope of the linear relationships predicted by the models gains relevance for larger deformations. As the specific volume decreases with the development of creep deformations, the slope of the semi-logarithm linear relationship $\psi_0/V_{current}$ increases, resulting in the differences observed in the figure.

6. Assessment of the model's potentials and limitations

Numerical simulation of load controlled undrained triaxial compression tests under constant rate of stress (termed as CRSS tests hereafter) are performed with *FLAC 2D* to further investigate the inability of the model to reproduce undrained failure conditions under load control conditions. A series of CRS tests is superimposed by two CRSS tests at different loading rates to interpret the response of the soil with continued loading. The CRS tests act as total axial strain rate contours and serve to highlight the continuous increase in strain rate of the CRSS tests. A value of 0.06 is initially assigned to the limit of volumetric viscoplastic strain $\varepsilon_{vol,m,Limit}^{vp}$.

The model parameters are the same as the ones specified in table 2. The soil has an OCR equal to 1.0 (isotropically consolidated to 600 kPa) and an initial void ratio of 1.5.

Figure 6 present the predicted $q - p'$ stress path obtained with the EVP model with the hyperbolic creep law for two CRSS undrained triaxial compression tests with an applied axial stress rate of 100 and 1000 kPa/day, assuming $\varepsilon_{vol,m,Limit}^{vp}$ equal to 0.06.

The contours of constant applied total axial strain rate, also presented in the figure, do not correspond to lines of constant Φ. Therefore, the isotach behaviour (unique relationship of $\Phi - p'_m - \varepsilon_{vol,m}$) is not directly explained by these contours. However, given that the viscoplastic scalar multiplier can be shown to be a function of the total applied strain rate, the contours serve as an indirect illustration of the continuous increase of Φ with loading. In addition, figure 7 is presented to aid the interpretation of the stress paths of these CRSS tests. The figure depicts the relationship between the size of the current loading surface p'_m and the associated volumetric strain $\varepsilon_{vol,m}$ (see equation 39).

The stress paths seem to follow closely a constant axial strain rate contour in the first few load increments, corresponding to 0.1 to 1% strain per day. This may be explained by the fact that the resulting axial strain rate due to incremental load is approximately constant in these increments.

The stress paths then cross contours of increasing axial strain rate with continued loading, which is due to the higher rate of increase of the viscoplastic scalar multiplier of the CRSS tests compared to that of the CRS tests (figure 7).

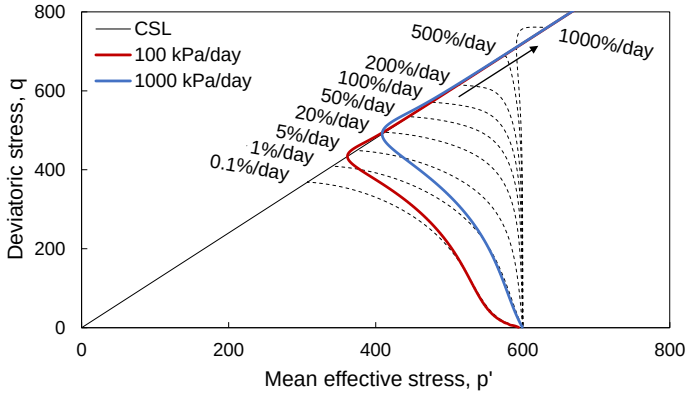

Figure 6 – Hyperbolic prediction of undrained triaxial compression CRS and constant rate of stress tests with $\varepsilon_{vol,m,Limit}^{vp}$ set equal to 0.06 for a NC sample (isotropically consolidated to 600 kPa) in $q - p'$ space (stress values in kPa)

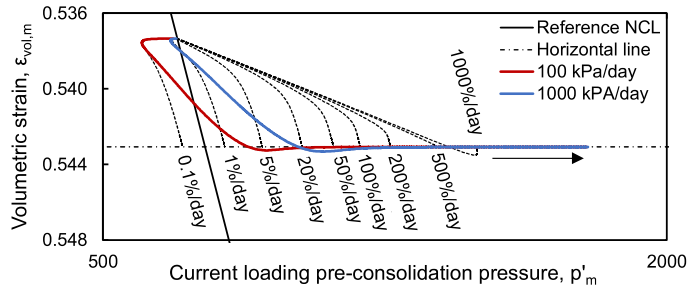

Figure 7 – Hyperbolic prediction of undrained triaxial compression CRS and constant rate of stress tests with $\varepsilon_{vol,m,Limit}^{vp}$ set equal to 0.06 for a NC sample (isotropically consolidated to 600 kPa) in $\varepsilon_{vol,m} - p'_m$ space (stress values in kPa)

The stress paths eventually reach the CSL but, because of the assumed uniqueness of the stress-strain-strain rate relationship, the continued increase in strain rate force the stress state to travel upwards on the line, increasing the undrained

shear strength. An overshoot is observed just before the stress paths join the CSL, coinciding with the dislocation of the stress states of the CRSS tests slightly under the dashed-dotted horizontal line illustrated in figure 7, which defines the critical state for the CRS tests.

It is not clear why the stress states of the CRSS tests dislocated under the horizontal line in $\varepsilon_{vol,m} - p'_m$ space and overshot the CSL in $q - p'$ space. The author suggests this occurs due to the transition of soil behaviour predicted by the model. Soil behaviour is initially contractive: the volumetric strain associated to the current loading surface increases and the stress paths depicted in $q - p'$ space tend towards decreasing values of mean effective stress. However, it is likely that the drastic increase in strain rate in the imminence of soil failure causes an increase of the soil apparent OCR, changing the behaviour of the soil from contractive to dilative. Consequently, the stress paths in $q - p'$ space bend to the right to comply with the change in soil behaviour, overshooting the CSL. In addition, it is possible to observe the decrease in $\varepsilon_{vol,m}$ in $\varepsilon_{vol,m} - p'_m$ space, such that after overshooting the soil state approaches the critical state line from the dilatant side.

Figure 8 gives the same CRSS tests plotted in $q - \varepsilon_a$ space.

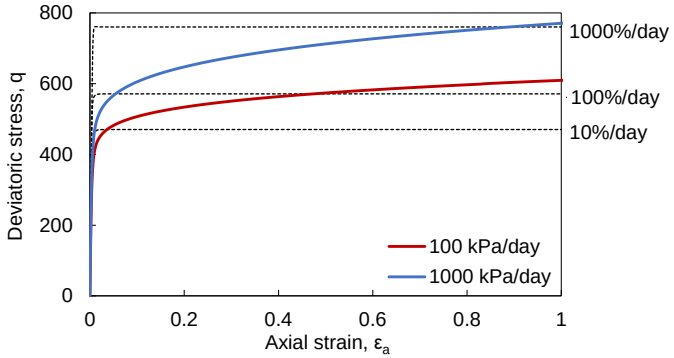

Figure 8 – Hyperbolic prediction of undrained triaxial compression CRS and constant rate of stress tests with $\varepsilon_{vol,m,Limit}^{vp}$ set equal to 0.06 for a NC sample (isotropically consolidated to 600 kPa) in $q - \varepsilon_a$ space (stress values in kPa)

The intersection of the CRSS stress paths with the contours of constant axial strain rate demonstrates the gain of the undrained shear strength with strain rate. As referred in section 5, the increase in the vertical spacing between contours of axial strain rate is a function of the limit of volumetric viscoplastic strain. Take the contours of 10%, 100% and 1000% strain per day for example, if the limit of volumetric viscoplastic strain is set to a larger value, the increase in the vertical spacing between these contours will be smaller and the contours would correspond to lower values of deviatoric stress compared to the ones illustrated in the figure. Since the stress paths of the CRSS tests cross these contours, the resulting undrained shear strength increases would also be lower. Hence, the gain in undrained shear strength with strain rate is shown to be controlled by the limit of volumetric viscoplastic strain as well.

Figure 9 plots a series of relationships between the normalised strain rate $\Phi_{current}/\Phi_{ref}$ and the vertical distance of the current soil state to the reference NCL (associated to the reference viscoplastic scalar multiplier Φ_{ref}). The vertical distance is represented by d_{ref} hereafter, and this is negative for soil states located above the reference time line and positive for soil states located below the reference time line. Each relationship corresponds to a given value for the limit of volumetric viscoplastic strain and it gives an idea of the variation in the vertical spacing between lines of constant Φ in $\varepsilon_{vol} - \ln p'$ space. The value of the creep parameter ψ_0/V is changed to 0.01 exclusively to amplify the differences between the $\Phi_{current}/\Phi_{ref} - d_{ref}$ relationships.

The phenomenon of creep usually involves a range of strain rates that is slower than the reference strain rate (left part of figure 9). In this range, the hyperbolic model has the advantage in relation to the semi-logarithm model because it predicts non-linear creep behaviour with a limiting value at infinite creep time. By choosing the value of the limit of volumetric viscoplastic strain, one decides the maximum value for d_{ref} at infinite creep time.

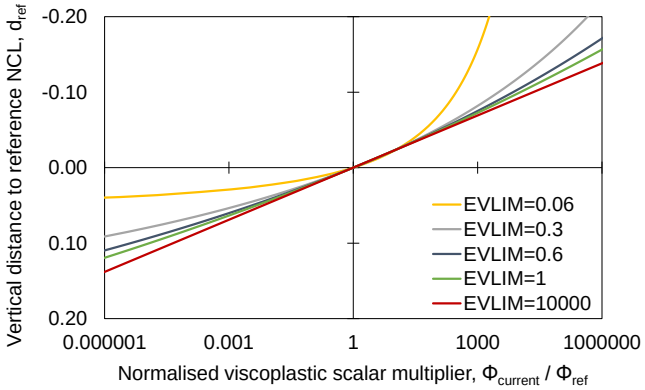

Figure 9 – $\Phi_{current}/\Phi_{ref} - d_{ref}$ relationships with values of $\varepsilon_{vol,m,Limit}^{vp}$ ranging from 0.06 to 10000

On the contrary, soil undrained failure under load controlled conditions is associated to a range of strain rates faster than the reference strain rate (right part of figure 9). The improvement of the adopted creep law for low strain rate values to recover good predictions of long term creep deformations (by adopting a value of $\varepsilon_{vol,m,Limit}^{vp}$ well below the value associated with the deformation required to reach zero void ratio) means that the creep law performs deficiently at higher strain rates predicting realistic gains in the soil undrained shear strength or apparent yield stress with increasing strain rate.

A good value for the limit of volumetric viscoplastic strain to obtain good estimates of creep deformations leads to a very poor model performance at very large strain rates that occur when analysing conditions close to failure. The semi-logarithm relationship (associated to a large value of the limit of volumetric viscoplastic strain) still predicts a continuous increase in the soil undrained shear strength (or apparent consolidation) for increasing large strain rate, however at a much slower rate. Therefore, the semi-logarithmic law is still unable to predict accelerating creep and undrained failure under load controlled conditions, but for large strain rates its performance is better than that of the hyperbolic law with a low value of $\varepsilon_{vol,m,Limit}^{vp}$.

A temporary improvement is to determine which behaviour one desires to model and calibrate the limit of volumetric viscoplastic strain according to the situation. Nevertheless, the problem of the continuous gain in the undrained shear strength with strain rate persists. It is necessary to implement changes in the formulation of the model in order to solve this issue. Some possible improvements are discussed in section 7.

7. Conclusion and suggestion for future works

An elastic-viscoplastic constitutive model based on the overstress theory was implemented. It incorporates: (i) a versatile surface proposed by Lagioia et al. [38]; (ii) Van Eekelen's (1980) failure criterion in the deviatoric stress space to define the slope of the critical state line under different shear conditions and (iii) either a semi-logarithm and hyperbolic creep law to characterise the delayed deformation of the soil under isotropic stress conditions.

The effects of isotach viscosity were clearly visible in the numerical predictions of constant rate of strain tests. Soils subjected to faster applied strain rates presented larger pseudo-elastic regimes, higher effective stresses and undrained shear strengths for the same level of strains. The observed effects were also permanent as long as straining was kept constant.

Because the constitutive model predicts a unique stress-strain-strain rate relationship it is unable to predict tertiary

accelerating creep, as this would require that various increasing strain rates can occur at a given stress-strain state. Therefore, the model fails to predict undrained shear failure under load controlled conditions. Some numerical simulations of constant rate of stress tests were therefore performed to assess this issue. The results showed that the strain rate increased drastically in the imminence of soil failure (when stress state approaches the CSL) and, owed to the isotach behaviour and the formulation of the model, a continuous gain in the undrained shear strength was predicted. Stress state dislocated upwards on the CSL in $q - p'$ space. An overshoot was observed when stress state reached the CSL. The author suggests that it was likely due to the change in soil behaviour (from contractive to dilative).

A sensibility analysis of the limit of volumetric viscoplastic strain during constant rate of stress undrained triaxial compression tests was then performed. The results show that, though the model performance is often improved in the range of the low strain rates, for example to estimate long term creep deformations, by setting a relative small value to the limit of volumetric viscoplastic strain to mimic a non-linear creep law, such values of $\varepsilon_{vol,m,Limit}^{vp}$ leads to poor model performances for high strain rates. For small values of $\varepsilon_{vol,m,Limit}^{vp}$ the model predicts unrealistic high gains in the undrained shear strength or apparent yield stress. During undrained shearing at constant stress rate, the rate of shear strength increase during continued straining was higher for smaller values of $\varepsilon_{vol,m,Limit}^{vp}$. In this respect, the parameter should be set to the maximum possible value to achieve the minimum rate of increase in the undrained shear strength, leading to predictions identical to that of the semi-logarithm model.

The author concluded the thesis by suggesting a temporary measure to this issue: the user should first determine which behaviour desires to model in order to calibrate the limit of volumetric viscoplastic strain according to that behaviour. However, the problem persists as the semi-logarithm model still predicts a continuous increase in the undrained shear strength with increasing strain rate.

Two possible improvements to the current model are: (a) the definition of an upper limit of volumetric viscoplastic strain for increasing strain rates. The resulting $\Phi_{current}/\Phi_{ref} - d_{ref}$ relationship in figure 9 would be depicted similarly to an S shape; (b) incorporation of temperature dependency. For more details, please refer to the main document.

8. References

[1] Tatsuoka, F., et al. *Some new aspects of time effects on the stress-strain behaviour of stiff geomaterials*. in *2nd Int. Conf. Hard Soils and Soft Rock*. 2000.

[2] Tatsuoka, F. *Effects of viscous properties and ageing on the stress-strain behaviour of geomaterials*. in *Geomechanics-Testing, Modeling, and Simulation. Proceedings of the GI-JGS workshop*. 2004. Boston.

[3] Sorensen, K.K., B.A. Baudet, and F. Tatsuoka. *Coupling of ageing and viscous effects in an artificially structured clay*. in *Soil Stress-Strain Behavior: Measurement, Modeling and Analysis*. 2007. Springer Netherlands.

[4] Bodas Freitas, T.M., *Numerical modelling of the time dependent behaviour of clays*. 2008, Imperial College, University of London.

[5] Leroueil, S. and M.E.S. Marques. *Importance of strain rate and temperature effects in geotechnical engineering*. in *Measuring and modeling time dependent soil behavior*. 1996. ASCE.

[6] Lacerda, W.A. and W.N. Houston. *Stress relaxation in soils*. in *Proceedings of 8th International Conference on Soil Mech. Found. Eng*. 1973.

[7] Murayama, S., K. Michihiro, and T. Sakagami, *Creep characteristics of sand.* Soils and foundations, 1984. 24(5).

[8] Di Prisco, C. and S. Imposimato, *Time dependent mechanical behaviour of loose sands.* Mechanics of Cohesive-frictional Materials, 1996. 1(1): p. 45-73.

[9] Lade, P.V. and C.-T. Liu, *Experimental study of drained creep behavior of sand.* Journal of Engineering Mechanics, 1998. 124(8): p. 912-920.

[10] Di Benedetto, H., F. Tatsuoka, and M. Ishihara, *Time-dependent shear deformation characteristics of sand and their constitutive modelling.* Soils and foundations, 2002. 42(2): p. 1-22.

[11] Kuhn, M.R. and J.K. Mitchell, *New perspectives on soil creep.* Journal of Geotechnical Engineering, 1993. 119(3): p. 507-524.

[12] Mesri, G., *Coefficient of secondary compression.* Journal of Soil Mechanics & Foundations Div, 1973. 99(1): p. 123-137.

[13] Mesri, G. and A. Castro, *Ca/Cc concept and K0 during secondary compression.* Journal of Geotechnical Engineering, 1987. 113(3): p. 230-247.

[14] Mesri, G. and P.M. Godlewski, *Time-and stress-compressibility interrelationship.* Journal of Geotechnical and Geoenvironmental Engineering, 1977. 103(ASCE 12910).

[15] Leroueil, S., et al., *Stress-strain-strain rate relation for the compressibility of sensitive natural clay Geotechnique.* Géotechnique, 1985. 35(2): p. 159-180.

[16] Singh, A. and J.K. Mitchell, *General stress-strain-time function for soils.* Journal of Soil Mechanics & Foundations Div, 1968. 94(1): p. 21-46.

[17] Yin, J.H., *Non-linear creep of soils in oedometer tests.* Geotechnique, 1999. 49(5): p. 699-707.

[18] Tavenas, F., et al., *Creep behaviour of an undisturbed lightly overconsolidated clay.* Canadian Geotechnical Journal, 1978. 15(3): p. 402-423.

[19] Bjerrum, L., *Seventh Rankine Lecture. Engineering geology of Norwegian normally-consolidated marine clays as related to settlements of buildings.* Géotechnique, 1967. 17(2): p. 81-118.

[20] Arulanandan, K., C.K. Shen, and R.B. Young, *Undrained creep behaviour of a coastal organic silty clay.* Geotechnique, 1971. 21(4): p. 359-375.

[21] Akai, K., T. Adachi, and N. Ando, *Existence of a unique stress-strain-time relation of clays.* Soils and Foundations, 1975. 15(1): p. 1-16.

[22] Vialov, S.S. and A.M. Skibitsky. *Problems of the rheology of soils*. in *Proceedings of the 5th International Congress on Soil Mechanics and Foundation Engineering*. 1961.

[23] Murayama, S. and T. Shibata. *Rheological properties of clays*. in *Proc. 5th Int. Conf. on Soil Mechanics and Foundation Engineering*. 1961.

[24] Tatsuoka, F. *Inelastic deformation characteristics of geomaterial*. in *Soil Stress-Strain Behavior: Measurement, Modeling and Analysis*. 2006. Geotechnical Symposium in Roma.

[25] Augustesen, A., M. Liingaard, and P.V. Lade, *Evaluation of time-dependent behavior of soils.* International Journal of Geomechanics, 2004. 4(3): p. 137-156.

[26] Tavenas, F. and S. Leroueil. *Effects of stresses and time on yielding of clays*. in *Proceedings of the 9th International Conference on Soil Mechanics and Foundation Engineering*. 1977.

[27] Matsushita, M. *Time effects on the prepeak deformation properties of sands*. in *Proc. Second Int. Conf. on Pre-Failure Deformation Characteristics of Geomaterials, IS Torino'99*. 1999. Balkema.

[28] Enomoto, T., et al. *Viscous property of granular material in drained triaxial compression*. in *Soil Stress-Strain Behavior: Measurement, Modeling and Analysis, Proc. of Geotechnical Symposium in Roma*. 2006.

[29] Liingaard, M., A. Augustesen, and P.V. Lade, *Characterization of models for time-dependent behavior of soils.* International Journal of Geomechanics, 2004. 4(3): p. 157-177.

[30] Kavazanjian, E. and J.K. Mitchell. *A general stress-strain-time formulation for soils*. in *Proc. 9th ICSMFE*. 1977.

[31] Yin, J.H. and J. Graham, *Viscous–elastic–plastic modelling of one-dimensional time-dependent behaviour of clays.* Canadian Geotechnical Journal, 1989. 26(2): p. 199-209.

[32] Yin, J.H. and J. Graham, *Equivalent times and one-dimensional elastic viscoplastic modelling of time-dependent stress-strain behaviour of clays.* Canadian Geotechnical Journal, 1994. 31(1): p. 42-52.

[33] Perzyna, P., *On the propagation of stress waves in a rate sensitive plastic medium.* Zeitschrift für Angewandte Mathematik und Physik (ZAMP), 1963. 14(3): p. 241-261.

[34] Adachi, T., F. Oka, and M. Mimura, *Mathematical structure of an overstress elasto-viscoplastic model for clay.* Soils and Foundations, 1987. 27(3): p. 31-42.

[35] Yin, J.H., J.G. Zhu, and J. Graham, *A new elastic viscoplastic model for time-dependent behaviour of normally and overconsolidated clays: theory and verification.* Canadian Geotechnical Journal, 2002. 39(1): p. 157-173.

[36] Bodas Freitas, T.M., D.M. Potts, and L. Zdravkovic, *A time dependent constitutive model for soils with isotach viscosity.* Computers and Geotechnics, 2011. 38(6): p. 809-820.

[37] Bodas Freitas, T.M., D.M. Potts, and L. Zdravkovic, *Implications of the definition of the Φ function in elastic-viscoplastic models.* Géotechnique, 2012. 62(7): p. 643.

[38] Lagioia, R., A.M. Puzrin, and D.M. Potts, *A new versatile expression for yield and plastic potential surfaces.* Computers and Geotechnics, 1996. 19(3): p. 171-191.

[39] Van Eekelen, H.A.M., *Isotropic yield surfaces in three dimensions for use in soil mechanics.* International Journal for Numerical and Analytical Methods in Geomechanics, 1980. 4(1): p. 89-101.

[40] Bardet, J.-P. and W. Choucair, *A linearized integration technique for incremental constitutive equations.* International Journal for Numerical and Analytical Methods in Geomechanics, 1991. 15(1): p. 1-19.

[41] Sorensen, K.K., *Influence of viscosity and ageing on the behaviour of clays*. 2006, University College of London.